

 **DOR: 20.1001.1.27170314.2021.10.1.6.5**

Research Paper

A Numerical Investigation the Effects of the Voltage on the Displacement and Stress of Copper-based Ionic Polymer-Metal Composites

Hamid Soleimanimehr^{1*}, Amin Nasrollah²

¹Assistant Professor of Mechanical Engineering, Department of mechanical engineering, Science and Research Branch, Islamic Azad University, Tehran, Iran

²Bsc. of Mechanical Engineering, Department of Mechanical Engineering, Science and Research Branch, Islamic Azad University, Tehran, Iran

*Email of corresponding author: soleimanimehr@srbiau.ac.ir

Received: April 27, 2021; Accepted: June 17, 2021

Abstract

Ionic polymer material composites (IPMCs) are a group of polymeric material which deform by applying voltage and the movement of cations of polymer; it should be mentioned that the finite element method using electromechanics equations can be used to analyze these types of problem and measure the deformation. This phenomenon can causes bending and internal stress. This research, it is tried to investigate the displacement and stress of IPMC by modeling and finite element method analysis. Firstly, a 2D IPMC is designed; then the materials are applied which are cooper for the electrodes and Nafion for the polymeric core. After applying boundary conditions and meshing, the results have been analyzed by the finite element method. It is found that the relation between voltage and its effect on the bending displacement of IPMC is direct. The conclusions include the maximum displacement of IPMC membrane under the voltage of 5V is 0.42 mm and the maximum Von Mises stress on the electrode is gained 3.29×10^{16} (N/m²).

Keywords

Ionic-polymer-metal Composites, Finite Element Method, Voltage, Displacement, Smart Material, MEMS

1. Introduction

Ionic polymer-metal composites (IPMCs) are a group of electroactive polymers (EAPs) that can be used as either an actuator or a sensor [1]. Recently, IPMCs have received significant attention; this is due to their abilities such as low working voltage [2], high sensitivity, natural polarity, large deflection [3]. Also, ability to work in wet and dry environments. These composites have been used in biomimetic machines, biomedicine, flexible sensing, and micro-electro-mechanical system (MEMS) [4]; for instance, drug-release devices, an active fin, active catheter-guide-wire maneuvering, jellyfish-like under-water microrobot, and refreshable braille display. Numerous actuator mechanisms such as magnetic, piezoelectric, electrostatic, electrohydrodynamic, magnetohydrodynamic, are used for the valves in the 3D printers. This is a prevalent way for manufacturing implants and artificial cells to help patients in biomedical engineering [5]. Despite their benefits, they also have

disadvantages; this includes operation period, low lifetime [6], working in dry environments expose IPMC actuators to water shortages, which results in poor performance of the actuator. Also, IPMCs cannot produce very large forces. They can produce forces in the range of $10^{-3} N$ to $10^{-1} N$ [7]. IPMCs are constructed from a polymeric membrane and two conductive electrodes. These will be discussed in more detail in the following parts. Nafion is the polymeric membrane used in our study is composed of sulfonated polyimide (SPI) nanofibers. they have high proton conductivity at low relative humidity [8]. A CAE software is used to model the stress; also, it provides a graphical tool for analyzing the behavior of these membranes. Firstly, the physical model of the implicit differential equation is made to determine the share of each part [5]. Then the above-mentioned CAE method is used with the finite element method. Because of the high investment of the research, the study of cheap electrode material has become an important research direction in this field [9].

The main core material of these actuators is Nafion 117. The electrodes are made of copper. In the desired membrane, internal stress occurs under electrical voltage. A suitable model will be obtained from the model based on dominated terms. With the finite element method, the applied voltage can cause displacement and stress.

2. Material and methods

These composite actuators bend in response to low-voltage. Also, generate a voltage in response to bending [10]; as is shown in Figure 1. The force generated by IPMC depends on the actuator's size, thickness, and applied voltage. Therefore, a long IPMC can produce a large displacement, but it cannot generate a high force; whilst a short IPMC can produce a small displacement with a high force at the tip of the membrane [11].

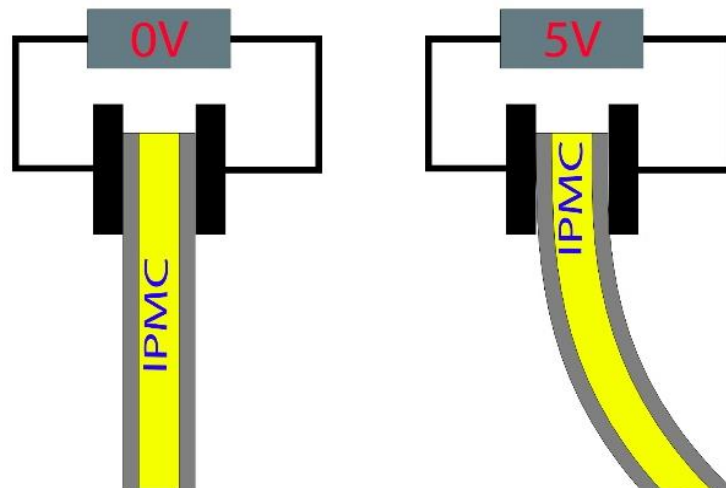


Figure 8: IPMC actuation: bending in response to the applied voltage at opposite polarities in left and right, and IPMC at rest in the middle

As it is mentioned earlier, IPMCs are fabricated like a sandwich structure containing an ion-exchange membrane and conductive electrodes. the polymeric membrane, Nafion, contains mobile hydrated cations, fixed anions, and water as solvents. The bending of an IPMC through the applied voltage makes the mobile cations move to the expanded region. This leads to the higher potential of the expanded side of the electrode, as is shown in Figure 2.

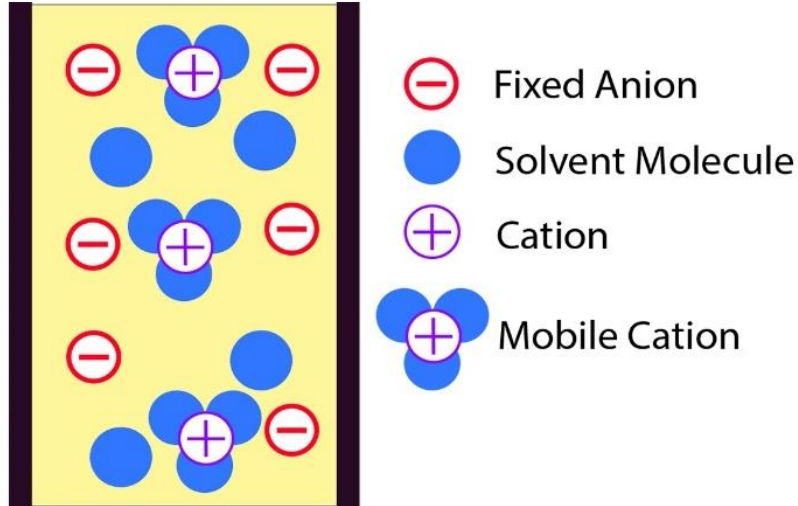


Figure 9. Ionic polymer-metal composite (IPMC) under a bending deformation

Constitutive equations were used to describe the processes that govern the actuation phenomenon of several physics-based IPMC sensing and actuation models. Proposed field equations relate the electric field “E”, electric displacement “D”, electric potential “ ϕ ”, charge density “ ρ ”, ion concentrations “ C^+ ” and “ C^- ”, and ion flux “J” within the polymer as follows in equations 1, 2, and 3:

$$E = \frac{D}{K_e} = \nabla\phi \quad (1)$$

$$\nabla \cdot D = \rho = F(C^+ - C^-) \quad (2)$$

$$\frac{\partial C^+}{\partial t} + \nabla \cdot J = 0 \quad (3)$$

By equation 4 where “F” is Faraday’s constant and “ K_e ” is the dielectric permittivity of the material, and “J” includes diffusion, migration, and convection terms:

$$J = -d \left(\nabla C^+ + \frac{C^+ F}{RT} \nabla \phi + \frac{C^+ \Delta V}{RT} \nabla p \right) + C^+ v \quad (4)$$

Where d is the ionic diffusivity, “R” is the gas constant, “T” is the absolute temperature, “p” is the fluid pressure and “v” is the free solvent velocity [10].

Table 1 illustrates dimensions of the IPMC actuator.

Table 5. Dimensions of IPMC actuator

Dimensions	Value	Unit
Length of IPMC	10	mm
The thickness of Nafion 117	0.07	mm
Thickness of electrode	1	um

In this part, the internal mechanism of the actuator is investigated under the influence of voltage. Firstly, the two-dimensional IPMC model was designed; then, the materials which are cooper for electrodes used in the valve and Nafion for the polymeric core. Properties of materials are shown in Table 2 and Table 3.

Table 6. Copper properties[12]

Property	Variable	Value	Unit
Relative permittivity	ε	1	1
Density	ρ	8960	Kg/m ³
Young's modulus	E	110×10^9	Pa
Poisson's ratio	ν	0.35	1

Table 7. Nafion properties[12]

Property	Variable	Value	Unit
Relative permittivity	epsilon	3502824824858.76	1
Density	ρ	3385	Kg/m ³
Young's modulus	E	0.5^9	Pa
Poisson's ratio	nu	0.487	1

The Electromechanics interface is the combination of solid mechanics and electrostatics with a moving mesh to model the deformation of electrostatically actuated structures [13]. Figure 3 shows 112,774 triangular mesh with average element quality of 0.8658.

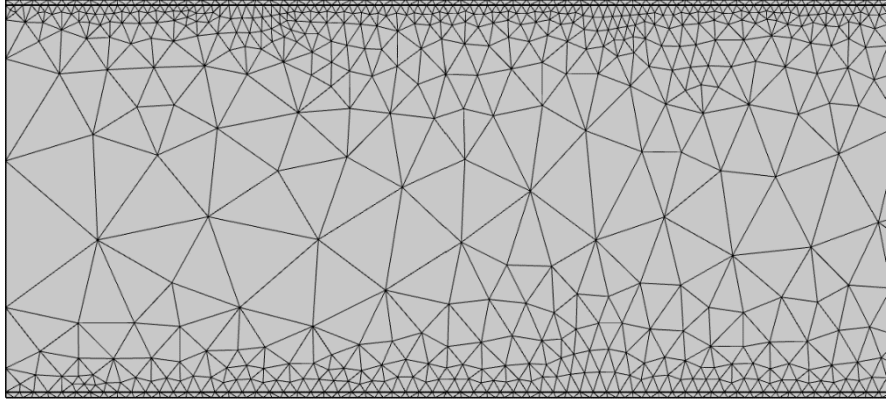


Figure 10. Meshing of IPMC actuator

The left side of the IPMC actuator is considered as a fixed constraint as given in equation 5; “ u ” is the displacement vector[13, 14].

$$u = 0 \quad (5)$$

The lower electrode is under 5V voltage, and the upper electrode is the terminal which means it is the ground input.

On the middle of the actuator, electronic conservation exists; the Charge Conservation node adds the equations for charge conservation according to Gauss’s law for the electric displacement field. It provides an interface for defining the constitutive relation defined by the relative permittivity in equations 6 and 7 [14].

$$E = -\nabla V \quad (6)$$

$$\nabla \cdot (\epsilon_0 \epsilon_R E) = \rho_V \quad (7)$$

Electrostatic uses equations 8 and 9; “ V ” is the changes of the molar volume of the solvent[15].

$$\nabla \cdot D = \rho_V \quad (8)$$

$$E = -\nabla V \quad (9)$$

Linear elastic material equations are equations 10 to 17; in these equations “ ϵ ” is strain, “ ∇u ” is the displacement gradient, “ F ” is force per volume, and “ T ” is the absolute temperature [16]:

$$\nabla \cdot (FS)^T + FV = 0 \quad (10)$$

$$F = l + \nabla u \quad (11)$$

$$F_{el} = FF_{inel}^{-1} \quad (12)$$

$$\epsilon = \frac{1}{2} [(\nabla u)^T + \nabla u + (\nabla u)^T \nabla u] \quad (13)$$

Briefly, in this part, first of all, the 2D IPMC actuator is designed and applied the materials to it which were copper and Nafion. Then boundary conditions were used, and meshing was done, and ultimately the finite element analysis.

3. Results and discussion

3.1 Investigation of displacement

The internal stress “ σ ” causes deformation in the IPMC actuator in a cantilever shape. For simplification of analysis, an intuitive method is adopted with element method software and finite element method for modeling the IPMC actuator. Displacement of IPMC membrane with an applied voltage of 5V is analyzed with the finite element method. It is shown in Figure 4.

The IPMC is actuated by applying a DC voltage that bends towards the cathode. Since the applying voltage increases, bending displacement increases. The maximum displacement of the IPMC membrane with a voltage of 5V is $420\mu m$. Figure 5 is the displacement diagram that shows the displacement’s value along the membrane.

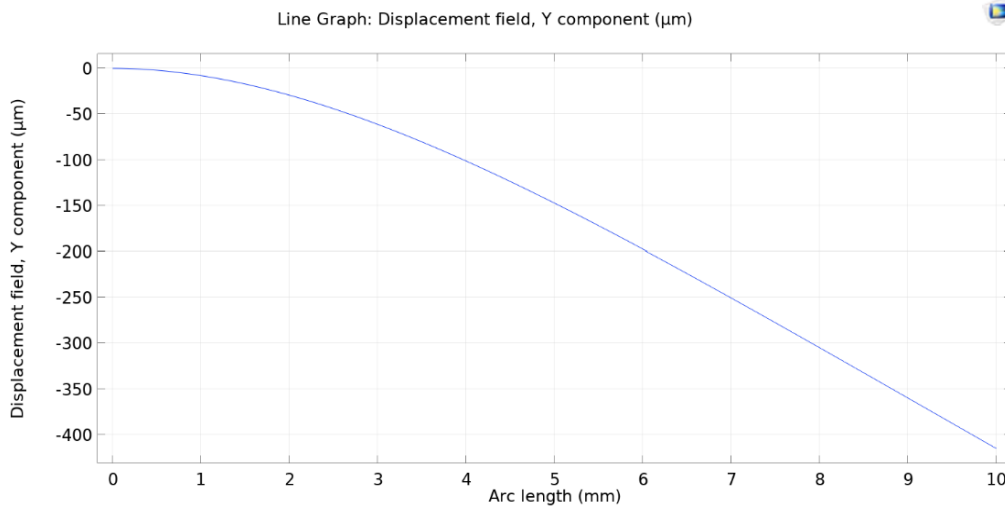


Figure 11. IPMC membrane deformation graph

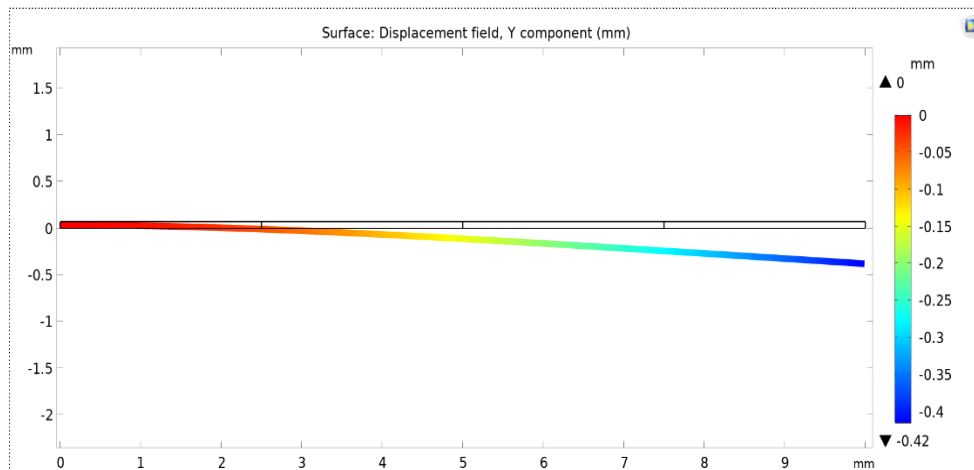


Figure 12. Displacement graphical diagram

3.2 Investigation of Stress

As cations in the Nafion membrane in an electric field are moving and concentrating in certain areas of IPMC, they take molecules of a solvent such as water with them. Locally, the concentration change

results in a change of the stress state. It can be decomposed that the total stress tensor into deviatoric and isotropic parts:

$$\sigma_{ij}^{tot} = \left(\sigma_{ij}^{tot} - \frac{1}{3} \delta_{ij} \sigma_{kk}^{tot} \right) + \frac{1}{3} \delta_{ij} \sigma_{kk}^{tot} \quad (14)$$

The hydrostatic pressure of the solvent due to the concentration change contributes to the isotropic part of the total stress tensor:

$$\frac{1}{3} \sigma_{kk}^{tot} = \frac{1}{3} \sigma_{kk} - p_c \quad (15)$$

$$\frac{1}{3} \sigma_{kk} = \frac{1}{3} (\sigma_{11} + \sigma_{22} + \sigma_{33}) \quad (16)$$

The equation is the isotropic part of the stress tensor related to the structural changes and “ p_c ” is the hydrostatic pressure of the solvent in Nafion due to the concentration change. Pressure “ p_c ” is zero in the electrode domains since it cannot be simulated any presence of cations there. For the Nafion domain, it is assumed that a linear relationship between the pressure “ p_c ” and concentration of free cations, “ c ”:

$$p_c = \beta_N \cdot (c - c_0) \quad (17)$$

Where “ β_N ” is a constant coefficient [6].

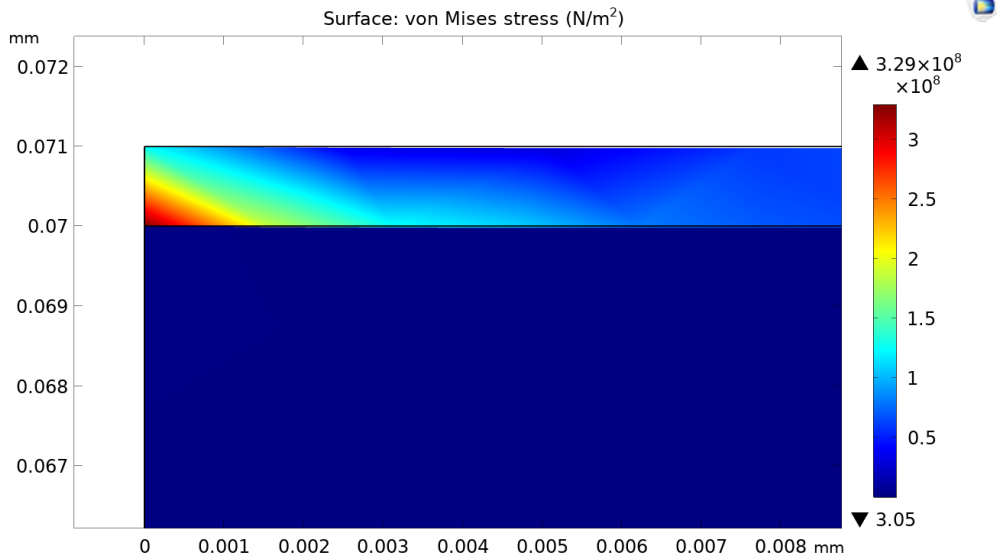


Figure 13. Von Mises stress on the electrode

As shown in Figure 6 the Von Mises stress on the electrode has the maximum value of 3.29×10^{16} (N/m²).

3.3 Stabilization

In this part, the deformation and stress diagram of the Nafion membrane of the IPMC membrane is under investigation as shown in Figure 7 and Figure 8.

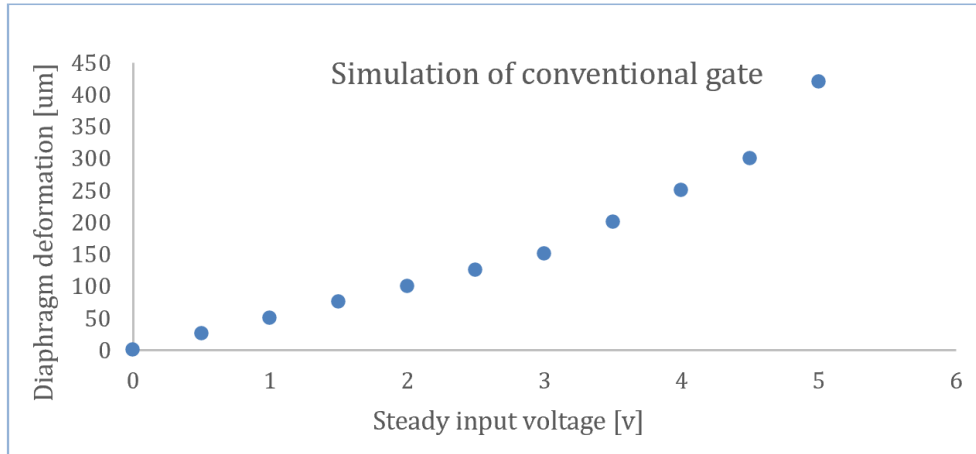


Figure 14. Deformation diagram of Nafion membrane in terms of input voltage

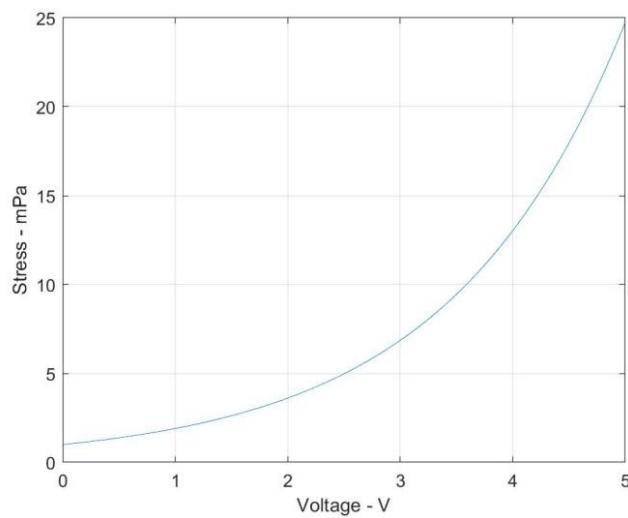


Figure 15. Stress diagram of Nafion membrane in terms of voltage

As shown, the Nafion does not have deformation at a voltage of 0V. When the voltage increases, the membrane starts bending. By the time voltage increases gradually, the size of deformation in order from first given point of the diagram is almost $50\mu\text{m}$ at 1V, $100\mu\text{m}$ at 2V, $150\mu\text{m}$ at 3V, $250\mu\text{m}$ at 4V, and $420\mu\text{m}$ at 5V.

It can be seen that there is no regular procedure for the increase of voltage and deformation. This is because of the nonlinear attitude of the electroactive polymer. The form of the diagram does not seem to be parabolic because of this irregular procedure. More evaluation can be obtained from checking the gradient of the diagram. The pressure gradient from 1st point to 2nd point is calculated at almost 25, from 2nd point to 3rd point it is about 28. This shows that in these parts the deformation changes follow a linear relation. This process remains stable until the voltage reaches 2V, where the 5th point is placed there is a slight decrease in the gradient. This decrease in that gradient can be observed for the 6th point as well as its previous point. At these points, due to the reduction of the slope, the deformation of the IPMC actuator is less than before. However, as the voltage rises again, this trend is reversed and the slope increases and in the last part of the diagram, deformation increases sharply

and reaches its maximum size, $420\mu m$. A is observed in our previous experimental test; however, it has a little error [16].

The diagram of stress in terms of voltage has a parabolic form which means that the relationship between stress and voltage of an IPMC actuator follows a quadratic equation. In this diagram as well as the deformation diagram, as the voltage increases, the stress rises which reaches its maximum amount $25Mpa$.

4. Conclusions

In this paper, the dependence of displacement and stress of an IPMC on voltage is studied. The finite element method analysis was analyzed by a finite element method software. Displacement is also studied and stress of both electrodes and membrane of IPMC actuator in individual diagrams. It was observed that in Nafion diagrams that deformation changes follow an irregular trend and the relation between stress and voltage is a parabolic relation. The results showed that the maximum displacement and stress in Nafion were in order $420\mu m$ and $25MPa$ and for electrode the stress was $3.29 \times 10^{16}Pa$. Eventually, the displacement of the IPMC membrane was found $420\mu m$. Respectively, it is obvious that the model studied in this paper can well reflect the relationship between voltage, stress, and displacement which can be useful for the later research of IPMC.

5. References

- [1] Yang, L., Zhang, D., Zhang, X., Tian, A. and Wang, X. 2020. Models of displacement and blocking force of ionic-polymer metal composites based on actuation mechanism. *Applied Physics A*. 126(5): 126-365.
- [2] Kinji, A., Naoya, M., Kohtaku, H., Yoshihiro, N., Toshiharu, M. and Zhi-Wei, L. 2004. Modeling of the electromechanical response of ionic polymer metal composites (ipmc). *Proc.SPIE*. 5385(1): 172-181.
- [3] Soleimanimehr, H. 2021. Analysis of the cutting ratio and investigating its influence on the workpiece's diametrical error in ultrasonic-vibration assisted turning. *Proceedings of the Institution of Mechanical Engineers, Part B: Journal of Engineering Manufacture*. 235(4): 640-649.
- [4] Wang, J., Wang, Y., Zhu, Z., Wang, J., He, Q. and Luo, M. 2019. The effects of dimensions on the deformation sensing performance of ionic polymer-metal composites. *Sensors*. 19(9): 1-12.
- [5] Nasrollah, A., Soleimanimehr, H. and Javangoroh, S. 2021. Finite element analysis assisted improvement of ionic polymer metal composite efficiency for micropump of 3d bioprinter. *Advanced Journal of Science and Engineering*. 2(1): 23-30.
- [6] Nguyen, T.T., Goo, N.S., Nguyen, V.K., Yoo, Y. and Park, S. 2008. Design, fabrication, and experimental characterization of a flap valve ipmc micropump with a flexibly supported diaphragm. *Sensors and Actuators A: Physical*. 141(2): 640-648.
- [7] Vokoun, D., He, Q., Heller, L., Yu, M. and Dai, Z. 2015. Modeling of ipmc cantilever's displacements and blocking forces. *Journal of Bionic Engineering*. 12(1): 142-151.

- [8] Makinouchi, T., Tanaka, M. and Kawakami, H. 2017. Improvement in characteristics of a nafion membrane by proton conductive nanofibers for fuel cell applications. *Journal of Membrane Science*. 530(1): 65-72.
- [9] Wang, F., Jin, Z., Zheng, S., Li, H., Cho, S., Kim, H.J., Kim, S. J., Choi, E., Park, J.-O. and Park, S. 2017. High-fidelity bioelectronic muscular actuator based on porous carboxylate bacterial cellulose membrane. *Sensors and Actuators B: Chemical*. 250(1): 402-411.
- [10] MohdIsa, W., Hunt, A. and HosseinNia, S.H. 2019. Sensing and self-sensing actuation methods for ionic polymer-metal composite (ipmc): A review. *Sensors (Basel)*. 19(18): 3967-4003.
- [11] Lee, S.G., Park, H., Pandita, S. and Yoo, Y. 2006. Performance improvement of ipmc (ionic polymer metal composites) for a flapping actuator. *International Journal of Control Automation and Systems*. 4(6): 748-755.
- [12] Nasrollah, A., Soleimanimehr, H. and Khazeni, H. 2021. Nafion-based ionic-polymer-metal composites: Displacement rate analysis by changing electrode properties. *Advanced Journal of Science and Engineering*. 2(1): 51-58.
- [13] COMSOL. 2021. Mems module user's guide, creating and analyzing mems models: The electromechanics interface. ed.
- [14] COMSOL. 2021. Mems module user's guide, the electrostatics interface: Charge conservation. ed.
- [15] Sakthi Swarrup, J. and Ranjan, G. 2015. Effect of mass loading on ionic polymer metal composite actuators and sensors. *Proc.SPIE*. 9430: 1-18.
- [16] Nasrollah, A. and Soleimanimehr, H. 2021. Electromechanical analysis on elasticity modulus of ionic-polymer-metal composites with platinum-based electrode and its comparison with experimental results. *The 6th International and 17th National Conference on Manufacturing Engineering (ICME)*.